by the superplumes lowers the viscosity of the asthenosphere (*8*, *26*), lubricating the motion of the lithospheric plates. In particular, this would allow for efficient slab pull in the Pacific and contribute to heating of the continental lithosphere under Africa (*6*, *27*). Most hot spots are derived from the two main upwellings. Exceptions may be hot spots in North America and perhaps Iceland, whose signature in the Q^{-1} models is lost below 400 km and whose deep or shallow origin has been the subject of vigorous debate (*7*, *28*, *29*). Because material from the large upwellings progressively mixes with the asthenosphere, the relation of the position of different hot spots with respect to the centers of the large upwellings may provide clues to their distinctive geochemical signatures (*30*), particularly in view of the noted correlation of the lower mantle superplumes with the Dupal anomaly (*31*).

Previous suggestions on the relation of major flood basalts to the two superplumes (*32*) and the stability of absolute hot spot locations (*33*) combined with the results of the present study indicate that the two large lower mantle upwellings may not be small instabilities in the present mantle convective system. In particular, the estimate of ~10% heat from the core carried by plumes (*34*) may need to be revised to account not only for hot spot flux but also for heat carried horizontally in the asthenosphere and eventually contributed to the ridge system.

References and Notes

1. G. Masters, S. Johnson, G. Laske, B. Bolton, *Philos. Trans. R. Soc. London Ser. A* **354**, 1385 (1996).
2. Y. J. Gu, A. M. Dziewonski, W.-J. Su, G. Ekström, *J. Geophys. Res.* **106**, 11169 (2001).
3. C. Mégnin, B. Romanowicz, *Geophys. J. Int.* **143**, 709 (2000).
4. Y. Fukao, S. Widiyantoro, M. Obayashi, *Rev. Geophys.* **39**, 291 (2001).
5. D. Bercovici, Y. Ricard, M. A. Richards, *Geophys. Monogr. Am. Geophys. Union 121* (American Geophysical Union, Washington, DC, 2000), p. 5.
6. B. Hager, R. W. Clayton, M. A. Richards, R. P. Comer, A. M. Dziewonski, *Nature* **313**, 541 (1985).
7. J. Ritsema, H. van Heijst, J. Woodhouse, *Science* **286**, 1925 (1999).
8. A. M. Forte, J. X. Mitrovica, *Nature* **410**, 1049 (2001).
9. M. Richards, B. H. Hager, N. H. Sleep, *J. Geophys. Res.* **93**, 7690 (1988).
10. S. I. Karato, *Geophys. Res. Lett.* **20**, 1623 (1993).
11. G. Nolet, F. A. Dahlen, *J. Geophys. Res.* **105**, 19043 (2000).
12. D. L. Anderson, *Science* **293**, 2016 (2001).
13. J. B. Minster, D. L. Anderson, *Philos. Trans. R. Soc. London Ser. A* **299**, 319 (1981).
14. For example, high-frequency body waves traveling through slabs arrive early but are defocused.
15. B. Romanowicz, *J. Geophys. Res.* **100**, 12375 (1995).
16. F. J. L. Reid, J. H. Woodhouse, H. H. van Heist, *Geophys. J. Int.* **145**, 695 (2001).
17. E. G. Roth, D. Wiens, L. M. Dorman, J. Hildebrand, S. Webb, *J. Geophys. Res.* **104**, 4795 (1999).
18. N. Suda, N. Shibata, Y, Fukao, *Geophys. Res. Lett.* **18**, 1119 (1991).
19. X. D. Li, B. Romanowicz, *J. Geophys. Res.* **101**, 22245 (1996).
20. The inversion involves comparison of observed waveforms of surface waves and body waves, with synthetics computed using normal mode theory. It proceeds in two steps. In the first step, waveform phases are aligned by constructing 3D elastic models of the mantle separately for *SH* (transverse component) and *SV* (vertical and longitudinal component) using the coupled-mode approach developed for *SH* models (*19*). In the second step, we invert for Q^{-1}, using three-component data and starting from a spherically symmetric reference Q^{-1} model (*35*), as well as the 3D velocity models obtained in the previous step. An additional variance reduction of ~7% is thus obtained. For this specific study, which is focused on the retrieval of Q^{-1} structure, velocity models are parametrized up to maximum spherical harmonics degree *smax* = 16 horizontally with the use of 16 B-splines vertically (throughout the mantle). The Q^{-1} models that have *smax* = 8 in the horizontal direction and 7 B-splines in the vertical direction use only fundamental and higher mode surface wave packets and are therefore restricted to the upper mantle. For crustal corrections, we use model Crust 5.1 (*36*) for velocities. We invert only for Q^{-1} structure below 80 km, correcting for shallow structure using information on Moho variations from Crust 5.1. Frequency dependence of Q^{-1} is not resolvable in the period range considered. Lateral variations in the lower mantle where Q^{-1} is low may be hard to detect.
21. N. D. Selby, J. H. Woodhouse, *Geophys. J. Int.* **142**, 933 (2000).
22. Our confidence in the stability of the Q^{-1} patterns derives from the comparison of models obtained independently using Z, L, or T component data, as well as bootstrapping and resolution experiments. The resolution experiments confirm our ability to distinguish structures in the uppermost 250 km from those at larger depth, whereas inversions using different components confirm that contamination by elastic effects does not dominate the observed patterns. [Y. Gung, B. Romanowicz, in preparation].
23. G. Ekström, A. M. Dziewonski, *Nature* **394**, 168 (1997).
24. J. P. Montagner, T. Tanimoto, *J. Geophys. Res.* **96**, 20337 (1991).
25. C. Gaboret, A. M. Forte, J. P. Montagner, *EOS* **82**, 47 (2001).
26. The existence of a low-viscosity channel under the lithosphere has been recognized for some time from modeling of glacial rebound as well as joint modeling of gravity and seismological data (*37*, *38*).
27. A. Nyblade, S. Robinson, *Geophys. Res. Lett.* **21**, 765 (1994).
28. C. Wolfe, I. T. Bjarnason, J. VanDecar, S. C. Solomon, *Nature* **385**, 245 (1997).
29. G. Foulger, D. G. Pearson, *Geophys. J.* **145**, F1 (2001).
30. S. R. Hart,, E. H. Hauri, L. A. Oschmann, J. A. Whitehead, *Science* **256**, 517 (1995).
31. P. Castillo, *Nature* **336**, 667 (1988).
32. K. Burke, *Eos* **82**, F1134 (2001).
33. W. J. Morgan, *Nature* **230**, 42 (1971).
34. N. Sleep, *J. Geophys. Res.* **95**, 6715 (1990).
35. J. J. Durek, G. Ekström, *Bull. Seismol. Soc. Am.* **86**, 144 (1996).
36. W. D. Mooney, G. Masters, G. Laske, *J. Geophys. Res.* **103**, 727 (1998).
37. G. Davies, M. Richards *J. Geol.* **100**, 151 (1992).
38. J. X. Mitrovica, A. M. Forte *J. Geophys. Res.* **102**, 2751 (1997).
39. A. Davaille, *Nature*, **402**, 756 (1999).
40. V. Babuška, J.-P. Montagner, J. Plomerova, N. Girardin, *Pure Appl. Geophys.* **151**, 257 (1998).

41. We thank A. Forte and a second reviewer for constructive comments, and A. Davaille for helpful discussions. Supported by NSF (grant no. EAR-0001965). It is BSL contribution no. 0205.

27 December 2001; accepted 8 March 2002

Evidence for an Ancient Osmium Isotopic Reservoir in Earth

Anders Meibom[1*] and Robert Frei[2]

Iridosmine grains from placer deposits associated with peridotite-bearing ophiolites in the Klamath mountains have extremely radiogenic $^{186}Os/^{188}Os$ ratios and old Re-Os minimum ages, from 256 to 2644 million years. This indicates the existence of an ancient platinum group element reservoir with a supra-chondritic Pt/Os ratio. Such a ratio may be produced in the outer core as a result of inner core crystallization that fractionates Os from Pt. However, if the iridosmine Os isotopic compositions are a signature of the outer core, then the inner core must have formed very early, within several hundred million years after the accretion of Earth.

Osmium has two radiogenic isotopes, ^{186}Os and ^{187}Os. ^{190}Pt decays to ^{186}Os with a half-life of ~449.4 billion years (Gy) (*1*), and ^{187}Re decays to ^{187}Os with a half-life of ~41.6 Gy (*2*, *3*). Therefore, the Os isotopic system may be used to track ancient fractionated highly siderophile element (HSE) reservoirs. For example, it has been argued that coupled enrichments in ^{186}Os and ^{187}Os in the deep-rooted Hawaiian and Noril'sk plume-derived lavas (*4*–*8*) are a signature of the outer core. In this model, radiogenic Os isotopic compositions have developed as a result of early fractionation of Os from Re and Pt during crystallization of the inner core that caused high Pt/Os and Re/Os elemental ratios to build up in the outer core. Because the lower mantle is expected to have low concentrations [~1 part per billion (ppb)] and the core high concentrations (>100 ppb) of HSEs (including Os, Re, and Pt), it would only require small amounts of outer core material to enter the lower mantle in order to imprint an outer core Os isotopic signature on plumes ascending from the core-mantle boundary (*4*–*9*).

[1]Geological and Environmental Sciences, 320 Lomita Mall, Stanford University, CA 94305-2115, USA. [2]Geological Institute, University of Copenhagen, Øster Voldgade 10, DK-1350 Copenhagen, Denmark.

*To whom correspondence should be addressed. E-mail: meibom@pangea.stanford.edu

However, inner core–outer core fractionation of Os, Re, and Pt remains poorly constrained partly because of a lack of experimental data on platinum group element solid-liquid metal partitioning coefficients relevant to the pressure-temperature regime and the largely unknown minor element composition of Earth's core (*10*), and partly because the timing of inner core crystallization is uncertain. Additional data are therefore needed to evaluate whether the Os isotopic signature of certain deep-rooted mantle plumes is an indication of an origin of these plumes at the core-mantle boundary.

We used the Stanford/USGS Sensitive High Resolution Ion Micro-Probe Reverse Geometry (SHRIMP RG) and negative thermal ionization mass spectroscopy (N-TIMS) (*11*) to measure the Os isotope compositions of 13 detrital, millimeter-sized iridosmine (Os-rich OsIrRu alloy) grains (Table 1) from placer deposits associated with the peridotite-bearing ophiolites in the Klamath Mountains in northern California and southwestern Oregon. It is generally agreed that peridotite-derived iridosmine grains may be robust representatives of the Os isotope reservoirs from which they form (*6*, *7*, *12*, *13*). Because of a very high Os concentration [>50 weight % (wt %)] and low Pt and Re concentrations (typically <0.1 wt %), the Os isotope composition of an iridosmine grain does not evolve over time but represents the composition of the Os reservoir at the time the grain formed. Furthermore, the highly refractory [melting temperature above 2000°C (*14*)] and inert nature of iridosmine makes subsequent exchange of Os in different environments (e.g., in the upper mantle, crust, and during alluvial transport) difficult.

One iridosmine sample (Josephine Creek) was collected from the heavy, black (chromite-rich) sands in Josephine Creek, which runs over the Josephine peridotite (*15*, *16*) and, via the Illinois River, into the Rogue River. Three of the analyzed grains were collected from placer deposits along the Rogue River (RR), which is a major drainage of the Josephine peridotite. Six of the grains were collected from placer deposits around Port Orford (PO) Oregon, near the ocean entry of the Rogue River. The last four iridosmine grains included in this study were collected during placer mining in northern California (NC), and the exact locality is not known. However, these samples are associated with placer deposits formed by erosion of peridotite-bearing ultramafic rocks (*12*, *17*).

The iridosmine grains are all characterized by distinctly sub-chondritic Pt/Os and Re/Os ratios (Table 1). Thus, in situ production of ^{186}Os and ^{187}Os has not changed the Os isotopic composition measurably after the grains formed. The measured $^{186}Os/^{188}Os$ ratios span a range from 0.1198368 ± 31 to 0.1198507 ± 48. Most are higher than the present-day chondritic $^{186}Os/^{188}Os$ value of 0.1198340 ± 20 (*6*); uncertainties are given as two standard deviations. The highest $^{186}Os/^{188}Os$ value measured (0.1198507 ± 48) is as high as the most radiogenic end-member of the Hawaiian lavas (0.1198475 ± 29) (*8*). The measured $^{187}Os/^{188}Os$ ratios in the iridosmine grains also span a wide range from 0.109534 ± 3 to 0.138880 ± 5 with a cluster of the grains falling within the 0.1240 to 0.1255 interval, indicating that substantial Os isotopic heterogeneity exists in the convective upper mantle. This inference is consistent with the large $^{187}Os/^{188}Os$ variations measured in peridotites drilled from the Izu-Bonin-Mariana forearc (*18*). Table 1 lists the calculated minimum ages for depletion of Re (T_{RD}) (*19*), which vary from ~256 million years (Ma) to ~2644 My, much older than the

Table 1. Os isotope composition and Pt/Os, Re/Os ratios of iridosmine grains. We report ±2 absolute standard deviations of the mean (σ_m) for the average of the replicate runs and ±2 absolute standard error of sample populations (values in parentheses). T_{RD} is the Re-depletion model age (*19*).

Sample	Pt/Os	Re/Os	$^{186}Os/^{188}Os$	$^{187}Os/^{188}Os$	γ_{Os}	T_{RD}(My)
Josephine Creek(a)			0.1198469(53)	0.124802(4)		
Josephone Creek(b)			0.1198482(57)	0.124855(9)		
Average	<0.01	$<10^{-3}$	0.1198476(39)	0.124829(5)	−2.20	417
RR 41(a)			0.1198453(34)	0.117887(9)		
RR 41(b)			0.1198458(52)	0.117895(5)		
Average	<0.01	$<10^{-3}$	0.1198456(30)	0.117891(5)	−7.63	1437
RR 13	0.9	$<10^{-4}$	0.1198507(48)	0.125912(5)	−1.35	256
RR 17	0.1	$<10^{-4}$	0.1198501(28)	0.124201(4)	−2.69	510
PO 20(a)			0.1198376(43)	0.109528(7)		
PO 20(b)			0.1198374(71)	0.109573(7)		
PO 20(c)			0.1198392(30)	0.109517(5)		
PO 20(d)			0.1198392(34)	0.109519(5)		
Average	<0.01	$<10^{-4}$	0.1198384(22)	0.109534(3)	−14.18	2644
PO 25	<0.01	$<10^{-3}$	0.1198454(59)	0.122316(5)	−4.17	789
PO 15(a)			0.1198475(79)	0.124357(7)		
PO 15(b)			0.1198488(54)	0.124314(5)		
Average	<0.01	$<10^{-3}$	0.1198482(47)	0.124335(4)	−2.58	490
PO 19	0.1	$<10^{-4}$	0.1198372(41)	0.125127(5)	−1.96	373
PO 26(a)			0.1198465(35)	0.133122(10)		
PO 26(b)			0.1198441(49)	0.133157(12)		
Average	<0.01	$<10^{-3}$	0.1198453(30)	0.133140(8)	4.32	
PO 24(a)			0.1198472(36)	0.138586(5)		
PO 24(b)			0.1198496(43)	0.139174(10)		
Average	0.01	$<10^{-4}$	0.1198484(28)	0.138880(5)	8.81	
NC 22	0.1	$<10^{-3}$	0.1198426(62)	0.120425(8)	−5.65	1067
NC 15	0.3	$<10^{-3}$	0.1198475(61)	0.120762(8)	−5.38	1017
NC 6-1(a)			0.1198362(25)	0.123122(3)		
NC 6-1(b)			0.1198374(62)	0.123647(6)		
Average	0.04	$<10^{-4}$	0.1198368(31)	0.123384(3)	−3.33	631
NC 6-2	0.04	$<10^{-4}$	0.1198483(30)	0.123135(5)	−3.52	668

age of formation of the Josephine ophiolite (~160 My), for example (*16*). Because of their large spread in age, the iridosmine grains provide a unique set of constraints on the time-integrated evolution of the HSE reservoir from which they may be derived.

In order to evaluate the possibility that the radiogenic Os isotope signatures in the Hawaiian and Noril'sk lavas and the iridosmine grains studied here are a result of outer core involvement into the lower mantle, we have modeled the Os isotopic evolution of the outer core as a result of fractionation of Os, Re, and Pt into the inner core. Three models, shown as solid lines *a*, *b*, and *c* in Fig. 1, have been explored. These models differ in the way Os, Re, and Pt partitions into the inner core, expressed by the solid metal–liquid metal partition coefficients D_{Os}, D_{Re}, and D_{Pt}. Model *a* has $D_{Os} = 19$, $D_{Re} = 14$, and $D_{Pt} = 2.9$ (*7*, *8*). Model *b* has $D_{Os} = 28$, $D_{Re} = 19.6$, and $D_{Pt} = 2.9$. Model *c* has $D_{Os} = 36$, $D_{Re} = 23.3$, and $D_{Pt} = 2.9$. All three models are based on the assumption of an initially chondritic Os isotope starting composition [$(^{187}Os/^{188}Os)_i = 0.0962$; $(^{187}Re/^{188}Os)_{chon} = 0.43$; $(^{186}Os/^{188}Os)_i = 0.119823$; $(^{190}Pt/^{188}Os)_{chon} = 0.0016$) (*6*, *19*)] as well as the assumption that the inner core formed to its present size within the first 250 My after Earth's formation (*7*, *8*). Model *a* is based on partitioning coefficients derived from the fractional crystallization trends of the IIA suite of iron meteorites (*7*, *8*, *20*, *21*). This model evolves to the present-day Os isotope composition of the radiogenic end-member of the Hawaiian mixing line ($\gamma_{Os} = \sim 8$ and $^{186}Os/^{188}Os = \sim 0.119852$) but does not reproduce the radiogenic $^{186}Os/^{188}Os$ ratios of the vast majority of the iridosmine grains, which are more radiogenic in $^{186}Os/^{188}Os$. This demonstrates that, even with the assumption that the inner core grew to its present size within the first 250 My after Earth's formation, the outer core did not evolve to the highly radiogenic $^{186}Os/^{188}Os$ ratios of the iridosmine grains early enough in its evolution, using the partitioning coefficients of model *a*.

Models *b* and *c* show that in order for the outer core to evolve to the measured $^{186}Os/^{188}Os$ ratios of the iridosmine grains and to reach a present-day Os isotope composition that falls on the Hawaiian mixing line, D_{Os} and D_{Re} must be increased by 90% and 66%, respectively, over the IIA iron meteorite values. D_{Pt} is kept constant in both model *b* and *c*. On the basis of IIA iron meteorite data $D_{Pt} = 2.9$; i.e., it is close to unity (*20*, *21*). In order to substantially enhance the outer core Pt/Os ratio by changing D_{Pt}, it becomes necessary to fundamentally change the partitioning behavior of Pt by making $D_{Pt} < 1$. For that reason, D_{Pt} was not changed in these models. The solid metal–liquid metal partition coefficients estimated on the basis of the Os isotopic compositions of the iridosmine grains are in general agreement with the most recent results from experiments designed to emulate inner core–outer core crystallization (D_{Os}, 15 to 32; D_{Re}, 15 to 33; D_{Pt}, 1 to 3) (*10*).

If the inner core formed later than ~250 My after Earth's formation, the solid metal–liquid metal partition coefficients required to produce the radiogenic Os isotope compositions of the iridosmine grains would have to be very high, e.g. $D_{Os} > 50$. Such extreme partitioning of Os into the inner core would lower the Os concentration in the outer core by at least a factor of 20 compared with the bulk Os concentration of the core, which would make it difficult to transfer a strong radiogenic Os isotope signature across the core-mantle boundary into the lower mantle.

Two iridosmine grains have $^{187}Os/^{188}Os$ ratios higher than the present-day average chondritic value of 0.1275 and $^{186}Os/^{188}Os$ ratios higher than chondritic. For these to have formed, conditions must have been such that, in addition to an Os reservoir with elevated $^{186}Os/^{188}Os$, Os from a reservoir with very radiogenic $^{187}Os/^{188}Os$ was added to their source region. Such a component could be recycled oceanic basalt (*8*). The yellow arrow in Fig. 1 illustrates the effect of mixing 10 to 15% Os from a 2-Gy-old oceanic basalt (Os = 0.05 ppb, Re = 0.927 ppb, and Pt = 6.0 ppb) (*8*) into a mantle reservoir with an Os isotope composition similar to that of the largest cluster of iridosmine grains. This shows that it is conceivable that these two iridosmine grains have incorporated a component of recycled oceanic basalt.

In conclusion, if indeed the radiogenic Os in the iridosmine grains and in the Hawaiian and Noril'sk plume-derived lavas is a signature of the outer core, then the present-day Os isotopic composition of the outer core is substantially more radiogenic than previously thought. On the basis of the data presented here, the present-day outer core would have to have a $^{186}Os/^{188}Os$ ratio of at least 0.119870 and a $^{187}Os/^{188}Os$ ratio of at least 0.1436. However, other possible scenarios, such as whether reservoirs with radiogenic $^{186}Os/^{188}Os$ exist in the mantle that could be responsible for the observed Os isotopic signatures in the geographically unrelated deep-rooted plumes and the iridosmine grains, also need to be explored.

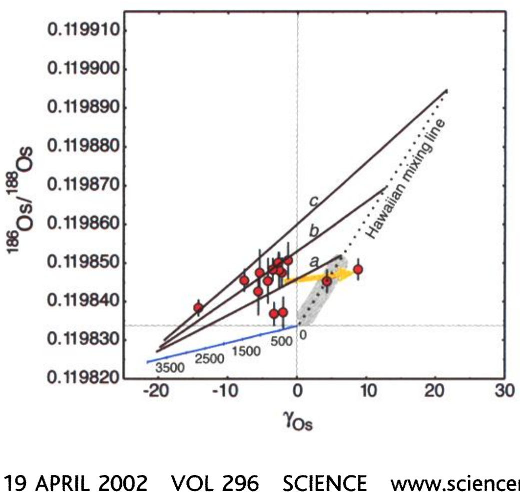

Fig. 1. Os isotope compositions of the iridosmine grains (red circles) and the Hawaiian and Noril'sk lavas (gray area). γ_{Os} is the percent deviation from the present-day chondritic $^{187}Os/^{188}Os$ ratio of 0.1276 (*22*). Blue line, the chondritic Os isotope evolution; numbers denote age from present in My. Solid black lines (*a*, *b*, and *c*) represent models of outer core Os isotopic evolution. Yellow arrow shows the shift mainly in γ_{Os} (i.e., $^{187}Os/^{188}Os$) as a result of mixing 10 to 15% Os from a 2-Gy-old oceanic basalt into an Os reservoir with an isotopic composition starting at $\gamma_{Os} = -2$ and $^{186}Os/^{188}Os = 0.119845$.

References and Notes

1. A. Brandon, J. E. Snow, R. J. Walker, J. W. Morgan, T. D. Mock, *Earth Planet. Sci. Lett.* **177**, 319 (2000).
2. M. I. Smoliar, R. J. Walker, J. W. Morgan, *Science* **271**, 1099 (1996).
3. J. J. Shen, D. A. Papanastassiou, G. J. Wasserburg, *Geochim. Cosmochim. Acta* **60**, 2887 (1996).
4. R. J. Walker *et al.*, *Geochim. Cosmochim. Acta* **58**, 4179 (1994).
5. R. J. Walker, J. W. Morgan, M. F. Horan, *Science* **269**, 819 (1995).
6. R. J. Walker *et al.*, *Geochim. Cosmochim. Acta* **61**, 4799 (1997).
7. A. D. Brandon, R. J. Walker, J. W. Morgan, M. D. Norman, H. M. Prichard, *Science* **280**, 1570 (1998).
8. A. D. Brandon, M. D. Norman, R. J. Walker, J. W. Morgan, *Earth Planet. Sci. Lett.* **174**, 25 (1999).
9. I. Puchtel, M. Humayun, *Geochim. Cosmochim. Acta* **64**, 4227 (2000).
10. D. Walker, *Geochim. Cosmochim. Acta* **64**, 2897 (2000).
11. Details of experimental procedures are available on *Science* Online at www.sciencemag.org/cgi/content/full/296/5567/516/DC1.
12. K. Hattori, S. R. Hart, *Earth Planet Sci. Lett.* **107**, 499 (1991).
13. T. Hirata, M. Hattori, T. Tanaka, *Chem. Geol.* **144**, 269 (1998).
14. R. D. Reiswig, J. M. Dickinson, *Trans. AIME* **230**, 469 (1964).
15. G. D. Harper, *Geol. Soc. Am. Bull.* **95**, 1009 (1984).
16. ______, K. Grady, J. Wakabayashi, *Geol. Soc. Am. Spec. Pap. 255* (1990), pp. 379–396.
17. W. B. Clark, *Pub. Calif. Div. Mines Geol.* **23**, 115 (1970).
18. I. J. Parkinson, C. J. Hawkesworth, A. S. Cohen, *Science* **281**, 2011 (1998).
19. S. B. Shirey, R. J. Walker, *Annu. Rev. Earth Planet. Sci.* **26**, 423 (1998).
20. J. W. Morgan, M. F. Horan, R. J. Walker, J. N. Grosman, *Geochim. Cosmochim. Acta* **59**, 2331 (1995).
21. J. H. Jones, A. Jurewicz, *Eos* **75**, 694 (1994).
22. R. J. Walker, M. F. Horan, J. W. Morgan, paper presented at the 11th Goldschmidt Conference, Hot Springs, VA, 20 to 24 May.

23. We thank the Field Museum of Natural History in Chicago (sample ID, M 8122), the Naturhistorisches Museum in Vienna (sample ID, A. a. 5432), and the Cornell University mineral collection (sample ID, Port Orford Oregon 22-8) for supplying samples. We are grateful to R. G. Coleman, C. P. Chamberlain, A. Brandon, R. J. Walker, and J. L. Wooden for inspiring and insightful discussions. We also wish to thank three anonymous reviewers. Their constructive reviews helped improve this manuscript.

18 December 2001; accepted 6 March 2002